europhysics
conference
abstracts

17th EPS Conference on

Controlled Fusion and Plasma Heating

Amsterdam, 25-29 June 1990

Editors: G. Briffod, Adri Nijsen-Vis, F.C. Schüller

Contributed Papers
Part II

Published by: European Physical Society

Series Editor: Prof. K. Bethge, Frankfurt/M.

Managing Editor: G. Thomas, Geneva

VOLUME 14 B Part II

GLOBAL, RESISTIVE STABILITY ANALYSIS IN AXISYMMETRIC SYSTEMS

A. Bondeson[a], G. Vlad[b], and H. Lütjens[a]

[a]Centre de Recherches en Physique des Plasmas, Ass. Euratom-Confédération Suisse Ecole Polytechnique Fédérale de Lausanne, 21 Av. des Bains CH-1007 Lausanne, Switzerland.

[b]Associazione Euratom-ENEA sulla Fusione, C.R.E. Frascati, C.P. 65 - 00044 - Frascati, Rome, Italy.

1.INTRODUCTION

Numerical codes such as ERATO [1] and PEST [2] have played an important role in developing the understanding of ideal-MHD stability for tokamaks. These codes solve the linearized ideal-MHD eigenvalue problem without any ordering assumptions. For resistive MHD, similar codes have been developed only recently [3]. Under a collaboration between the CRPP Lausanne and ENEA Frascati, we have developed a resistive spectral code, MARS (MAgnetohydrodynamic Resistive Spectrum), for the full compressional MHD equations in two-dimensional geometry. Axisymmetric equilibria are computed by the cubic Hermite element code CHEASE, which allows specification of the pressure p and toroidal field, $T = RB_\phi$, or the surface averaged toroidal current, $I' = \langle J_\phi \rangle$, as functions of the poloidal flux ψ. The two codes use flux coordinates (s, χ, ϕ), where $s = (\psi/\psi_{edge})^{1/2}$ is the radial variable, ϕ the geometrical toroidal angle, and χ the poloidal angle, specified by choosing the Jacobian, J. MARS Fourier decomposes the components of v and **B** in χ and uses a finite difference scheme in the radial direction.

Here, we present results for a number of resistive instabilities where toroidal effects play an important role. All calculations are made with a fixed, and except where explicitly stated otherwise, circular boundary.

2. INTERNAL KINK

The properties of the n=1, internal kink mode differ strongly between a torus and a cylinder. For $q_0 < 1$, $q_{edge} > 1$, a finite aspect ratio cylinder is ideally unstable, independent of pressure, while the torus is *ideally* stable for $\beta_{pol} < \beta_{pcrit}$. At large aspect ratio, β_{pcrit} is independent of A = R/a, but depends on equilibrium profiles [4]. It has been shown recently [5,6] that at tight aspect ratio, even the *resistive* internal kink mode can be stable if the shear at the q=1 surface is sufficiently low. In Fig. 1 we show the growth-rate of the resistive internal n=1 mode as a function of aspect ratio for two different sequences of equilibria at zero β. The two sequences have different current profiles $I'(\psi)$ (both smooth functions of ψ) which are kept fixed, while the aspect ratio is varied. For Fig.1a, $I'(\psi)$ is monotonic, the q=1 radius is kept fixed at $r_{q=1} = 0.44a$, the central q is about 0.90 and the shear, $\hat{s} = r\, dq/dr$ at q=1, increases slightly with $\varepsilon_{q=1} = r_{q=1}/R$ from 0.20 to 0.25. Although the resistive growth-rate decreases with increasing ε, the resistive modes remain unstable down to very tight aspect ratio, $\varepsilon_{q=1} = 0.3$. The second sequence of equilibria (Fig. 1b) has less shear in the $q \le 1$ region and $dI'/d\psi = 0$ at the q=1 surface. Here $r_{q=1} = 0.62a$, $q_0 = 0.93$ and s ranges from 0.09 to 0.12, depending on aspect ratio. These equilibria are resistively stable for $\varepsilon_{q=1} > 0.25$. For $\eta < 10^{-6}$ and $\varepsilon_{q=1} < 0.15$, the growth-rates both in Fig. 1a and 1b follow the large-aspect-ratio scaling [6] for n=1 "m=1" tearing, $\gamma \propto \eta^{3/5}\, \varepsilon^{-8/5}$. For large η and small ε, the scaling is closer to that of the cylindrical resistive kink, $\gamma \propto \eta^{1/3}\, \varepsilon^{0}$. Triangularity, up to $\delta = 0.4$, has a negligible effect on the growth rates in the high-shear case, Fig.1a. In the case of lower shear (1b), triangularity is weakly stabilizing; $\delta = 0.3$ reduces the $\varepsilon_{q=1}$ needed for resistive stability from 0.25 to 0.21.

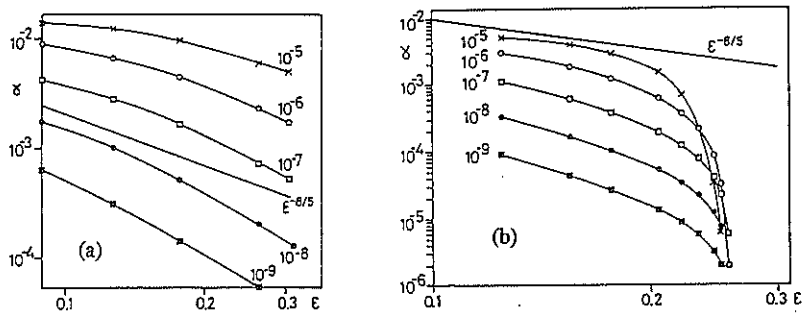

Fig. 1. Growth-rates of resistive internal kink mode as functions of aspect ratio for $\eta = 10^{-5}, 10^{-6}, 10^{-7}, 10^{-8}$, and 10^{-9}. (a) $\hat{s}_{q=1} \approx 0.2$, (b) $\hat{s}_{q=1} \approx 0.1$.

Generally, in tokamaks, $\varepsilon_{q=1} < 0.25$, and, from TEXTOR, q_0 as low as 0.7 has been reported [5]. Under such conditions, resistive stability requires a local reduction of the shear at the q=1 surface [5] and a non-monotonic current profile. Figure 2 shows resistive growth-rates for an equilibrium with finite pressure and where the shear has a local minimum near the q=1 surface. For these equilibria, $R/a = 2.5$, $q_0 \approx 0.7$, $q_{edge} \approx 2.4$, and $r_{q=1} \approx 0.51a$. We used a non-monotonic current profile $I'(\psi)$, and the shear profile for $\beta_{pol} = 0.13$ is shown in Fig. 2b. Figure 2a gives contours of equal growth-rate for $\eta = 10^{-7}$ as a function of β_{pol}, measured at the q=1 surface, and $q_i \equiv q(s=0.607)$, near the inflection point of q(s). Fig. 2a shows that the stable window in q_i is narrow and eventually shrinks to zero as β increases. Furthermore, the stable values of q_i increase with increasing β, which means that the q=1 surface moves inward into a region of somewhat higher shear. The apparent reason for this is that the ideal pressure driven mode is stabilized by global shear, and this effect competes with the requirement of low local shear for resistive stability. The resistive β-limit is therefore somewhat lower than the ideal one. The maximum value of $\beta_{pol}(q=1)$ reached with our profiles is 0.2, to be compared with the ideal limit of 0.3 for a parabolic q-profile [4].

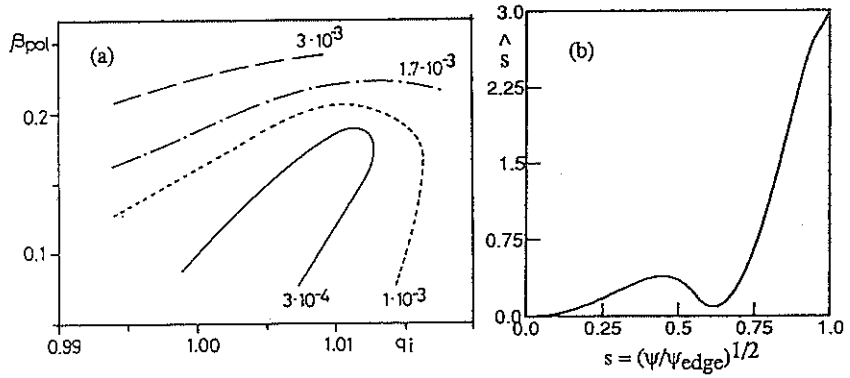

Fig. 2. (a) Growth-rate for resistive internal kink as a function of β_{pol} at q=1 and $q_i \equiv q(s=0.607)$, for a non-monotonic current profile with shear profile (b).

3. M ≥ 2 TEARING MODES AT FINITE BETA

Glasser, Greene and Johnson [7] showed analytically that the tearing mode is stabilized by favourable average curvature when β and $S = 1/\eta$ are sufficiently large. We have studied finite-β effects on the n=1 "m=2" tearing mode, using a current profile in the form of a rounded-off step-function, fixing A=2.5 and $q_0 = 1.5$ (strongly unstable to m=2 tearing in a cylinder) and varying the central β between 0.35 % and 2.45 %. (This made q_{edge} vary from 4.8 to 6.) The pressure at the edge was taken to be finite, at about 6 % of the central pressure p_0, while $p \approx 0.33\ p_0$ at the q=2 surface. The resistivity profile was inversely proportional to p. Figure 3a shows the real part of the growth rate as a function of central η for different β_0. Note that, for η above some value η_1,there are two purely growing modes which coalesce at $\eta = \eta_1$ and split into a pair with complex conjugate growth rates, which is unstable in a range $\eta_2 < \eta < \eta_1$, and finally becomes stable for $\eta < \eta_2$. The curves for different β in Fig 3 are almost identical if γ is scaled as $\beta^{3/2}$ and η as $\beta^{5/2}$, consistent with the simplified dispersion relation (88) for H = 0 in Ref.7. (For our equilibrium with $\beta_0 = 2.45$ %, in the notation of [7], $D_R \approx -0.16$ and $H \approx 0.08$ at the q=2 surface.) Clearly, high β is strongly stabilizing for resistive modes when the average curvature is favourable. Figure 3b shows the Fourier components of the perturbed magnetic field (with straight field-line Jacobian $J \propto R^2$)

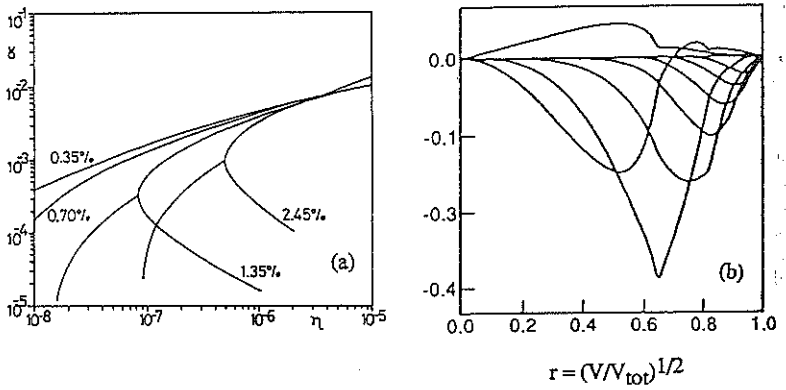

Fig.3 (a) Real part of growth-rate for "m=2", n=1 tearing mode for finite-β equilibria described in text. (b) Fourier components of $J\ \nabla s \cdot b$ for the near marginal mode at $\eta = 1 \times 10^{-7}$ and $\beta_0 = 2.45$ %.

4. LOW-N RESISTIVE BALLOONING

Resistive ballooning modes are driven by pressure gradients in regions of unfavourable local curvature, and the ideal stabilization by field bending is reduced by resistivity. The resistive ballooning modes are, however, stabilized at sufficiently high S and large sound speed by fluid compression [8,9]. From the analytical theory of Ref. 9, we find that the pressure necessary for stabilization of high-n resistive ballooning modes scales with resistivity and pressure gradients as $\Gamma p_{stab} \propto \eta^{1/2}\ (dp/dr)^2$, where Γ is the adiabatic index (usually set to 5/3). We have verified with MARS that this scaling holds also for n=1 and n=2 modes. The

scaling implies that resistive ballooning modes will generally be unstable near the plasma boundary, where p is small and η large, unless dp/dr goes sufficiently rapidly to zero. (This is why we added a base pressure of $0.06 p_0$ to separate tearing from resistive ballooning in Sec. 3.) It should be noted that resistive ballooning is stabilized in incompressible calculations where $\Gamma = \infty$. Fig. 4 shows the Fourier components of the velocity and magnetic field for an n = 2 resistive ballooning mode. The equilibrium has $q_0 = 1.02$, $q_{edge} = 2.5$, $\langle\beta\rangle = 2$ %, and a finite pressure gradient at the edge. The pressure at the edge has been raised to the point where the mode is marginally stable, $\beta_{edge} = 1.2 \times 10^{-3}$ with $\Gamma = 1$. The resistivity profile is given by $\eta(\psi)/\eta_0 = p_0/p(\psi)$, with $\eta_0 = 1 \times 10^{-7}$, and the real frequency of the mode is about $9 \times 10^{-3}\ \omega_A$. Figure 4 shows that the velocity perturbations have a short radial wave-length, and are confined to the edge region. It is noteworthy, however, that the magnetic perturbations penetrate with a long radial wave-length to the centre of the plasma. Another interesting property, that can be seen from the radial variation of the complex amplitudes, is that near the plasma edge, the perturbations propagate radially outward. The mode involves a large number of different poloidal Fourier components and is thus strongly ballooning. It appears justified to speculate that modes of this type are responsible for transport in the edge region of tokamaks, and that their magnetic perturbations may contribute to transport also in the interior.

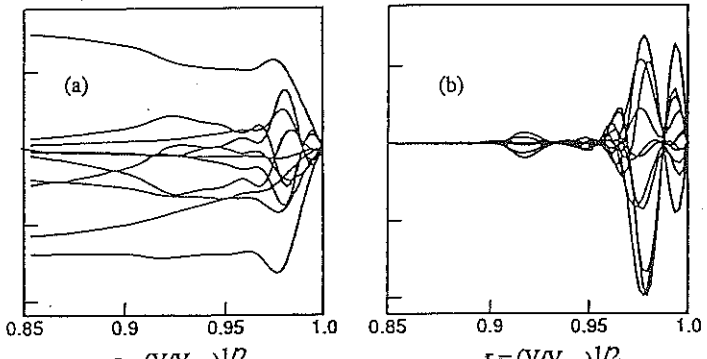

Fig. 4 Fourier components of radial magnetic field and velocity. (a) $J\ \nabla s \cdot b$ and (b) $\nabla s \cdot v$ over outer 8 % of the minor radius.

REFERENCES

1. R. Gruber, F. Troyon, D. Berger, et al, Comp. Phys. Comm. **21**, 323 (1981).
2. R.C. Grimm, J.M. Greene, and J.L. Johnson, Meth. Comp. Phys. **16**, 253 (1976): J. Manickam, R.C. Grimm, and R.L. Dewar, Comp. Phys. Comm. **24**, 355 (1981).
3. L.A. Charlton, J.A. Holmes, H.R. Hicks, et al, J. Comp. Phys. **63**, 107 (1986).
4. M.N. Bussac, R. Pellat, D. Edery and J.L. Soule, Phys. Rev. Lett. **35**, 1638 (1975).
5. H. Soltwish, W. Stodiek, J. Manickam, et al , IAEA Kyoto (1986),Vol I, p. 263.
6. J.A. Holmes, B.A. Carreras, and L.A. Charlton, Phys. Fluids B **1**, 788 (1989).
7. A.H. Glasser, J.M. Greene, and J.L. Johnson, Phys. Fluids **19**, 567 (1976).
8. T.C. Hender, B.A. Carreras, W.A. Cooper, et al. Phys. Fluids **27**, 1439 (1984).
9. J.F. Drake and T.M. Antonsen, Jr., Phys. Fluids **28**, 544 (1985).